DUAL ANTENNA HANDSETS DIVERSITY PERFORMANCE IN INDOOR PERSONAL COMMUNICATIONS

J. S. Colburn and Y. Rahmat-Samii
Department of Electrical Engineering
University of California, Los Angeles
Los Angeles, CA, USA 90095-1594
http://antlab.ee.ucla.edu

1. Introduction

The short-term fading caused by multipath propagation can be significant in indoor environments and in many cases is the limiting effect in wireless system performance. Antenna diversity is the process of selectively combining the signals received over multiple antennas and is one technique that can be used to help mitigate the effects of multipath fading.

This paper presents the experimental procedure used and results generated in a study to evaluate the diversity performance of three candidate dual antenna handset designs. The indoor Industrial, Scientific and Medical (ISM) frequency band (902-928 MHz) channel was of interest in this study, in particular nonline-of-sight indoor paths where multipath propagation results in the deepest signal fades. For comparison purposes, the diversity performance of two vertical orientated, horizontally spaced dipoles will also be presented.

2. Three Candidate Antenna Configurations

This work was undertaken to evaluate the diversity performance of three dual antenna configurations for a small transceiver handset. Figure 1 illustrates the configurations considered: (a) top mounted helix and back mounted planar inverted F antenna (PIFA); (b) side mounted PIFAs; (c) top mounted PIFA and flip monopole. The overall dimensions of the handset geometry considered are given in Figure 1 (c), with the specific antenna locations and dimensions for each design specified in Figures 1 (a), (b) and (c). In addition to the above described dual antenna handset geometries, the diversity performance of two vertically orientated dipoles with horizontal separation of 0.06 λ and 0.4 λ was evaluated.

The dual antenna handsets illustrated in Figure 1 achieve their overall diversity performance from all three types of antenna diversity: spatial, polarization and pattern. Consider the top mounted helix and back mounted PIFA structure shown in Figure 1 (a). These two antennas are displaced from each other (approximately 5 cm) and have different pattern and polarization characteristics, resulting in significant decorrelation between the two received signals. Similarly, the dual side mounted PIFA configuration illustrated in Figure 1 (b) achieves pattern and polarization diversity through physical element displacement as well as opposite orientation [1]. These same descriptions also apply to the top mounted PIFA and "flip" monopole handset of Figure 1 (c), although in this case a significantly larger element separation is used (approximately 15 cm).

3. Experimental Approach

A diagram of the equipment setup used to conduct the correlation measurements of the proposed dual antenna handset configurations is shown in Figure 2 [2]. The transmitter for these tests consisted of a sweep oscillator connected to a $\lambda/2$ dipole antenna. The source was operated in single-frequency mode at 915 MHz. The source output power was adjusted to 17 dBm, and the mismatch reflection coefficient of the transmitting dipole was measured to be under -10 dB at the frequency of interest.

On the receiver end, the antenna geometries described in Section 2, were used as antennas 1 and 2. The outputs of these antennas were amplified, then piped into separate spectrum analyzers. The noise floor of the spectrum analyzers was about -74 dBm so the preamplification of the signals was performed to increase the measurable fading range of the multipath signals. Placing the amplifiers in the RF path raised the noise floor about 10 dBm. The spectrum analyzers were put in zero span mode and centered on 915 MHz, for which the video output signals were proportional to the received power in dBm. The analog video output signals of the spectrum analyzers were then digitized and the data recorded on a personal computer. The digitizing rate used was approximately 72 samples per second per channel.

For each test run, the receiver was located in a typical laboratory room in the Engineering IV building on the UCLA campus while the transmitting antenna was moved along one of six predetermined paths at a constant speed. The paths were chosen such that there was no line-of-sight path. Three paths (1, 2 and 6) were located on the same floor as the receiver and three paths (3, 4 and 5) were located on the floor below the receiver. The Engineering IV building on the UCLA campus is a large office building of modern construction, consisting of individual offices, large open laboratories and cubical areas. The approximate floor dimensions are 67 m x 60 m. During each test run the transmitter was moved approximately 0.5 meters per second and the time length of each test run was 30 seconds. For movement at 0.5 meters per second and analog to digital sampling at 72 samples per second per channel, at 915 MHz this translates into approximately 47 samples per wavelength.

4. Results and Discussions

The demeaning of the measured data before calculation of the correlation is important to remove the slow-fades which result from propagation losses and are not a function of multipath. In this work, the slow fading nature of the signal was assumed to be a multiplicative factor and was extracted from the observed data by simply normalizing it with the *local* mean. Various time lengths were used to computed the local means and the effects on observed correlation studied [2]. For the experimental results in this study it was decided to use a two second time period to compute the local means.

A common model for indoor short term fading is that it follows a Rician or Rayleigh law [3]. In a pure multipath environment, where many equal amplitude and uniformly distributed phase replicas of the transmitted signal arrive at the receiver, the short term fading envelope will have a Rayleigh probability density function (PDF)

$$p(r) = \frac{r}{\sigma^2}\exp\left(-\frac{r^2}{2\sigma^2}\right) \tag{1}$$

where σ^2 is the mean signal strength and $r^2/2$ is the short term signal power. However, when there is line-of-sight or at least a dominant specular component, the short term fading envelope will have a Rician PDF

$$p(r) = \frac{r}{\sigma^2}\exp\left(-\frac{r^2+r_s^2}{2\sigma^2}\right)\mathrm{I_0}\left(\frac{rr_s}{\sigma^2}\right) \tag{2}$$

where I_o is the modified Bessel function of the first kind and order zero, σ^2 is the mean signal strength, $r^2/2$ is the short term signal power and $r_s^2/2$ is the power of the dominant component. Note, the Rayleigh distribution is a special case of the Rician distribution when $r_s = 0$. A commonly used notation for the dominant to multipath signal power ratio for the Rician distribution is

$$K = 10\ \log\frac{r_s^2}{2\sigma^2} \quad \mathrm{dB}. \tag{3}$$

For each of the test paths considered, the observed fading distributions were studied in order to determine the multipath nature of each path. A curve fitting was done to determine the *best* fit theoretical cumulative distribution functions (CDF) to each measured data set. The *best* fit to a theoretical CDF was determined in the minimum mean squared error sense between the measured CDFs and true Rician CDFs for K values between -5 to 15 dB in steps of 0.5 dB. A true Rayleigh CDF was also used in the test. In total 48 measurements were made for the 5 different dual antenna configurations over the 6 different paths. Figures 3 and 4 are example plots of the measured, *best* fit and Rayleigh CDFs for one of the measurements from paths 1 and 2 respectively.

From the measured CDFs it was seen that paths 1, 4, 5 and 6 exhibit strong multipath behavior (either a true Rayleigh or a Rician with a small value of K was the *best* fit). For path 2 the best fit Rician curves had much higher K values, indicating that this path had a fairly dominant component. The signals recorded on path 3 were very low in signal strength with many of the fades clipped by the noise floor of the experimental setup. Because of these facts the correlation data from paths 2 and 3 were not cosidered relevant.

Table 1 lists the computed correlation coefficients for the five different dual antenna configurations noted earlier for the test paths considered most relevant. From Table 1 one can see all three proposed dual antenna handset designs achieve diversity performance equal to or greater than that of two vertically orientated dipole antennas with 0.4 λ of horizontal separation. With maximal-ratio combining in a Rayleigh fading environment, it is possible to achieve 10 of the possible 12 dB of diversity gain of a dual branch system over a single channel system (assuming a 99% signal reliability criterion) with 0.6 branch correlation [4]. This fact and the data from these experiments indicate that the three proposed dual antenna handset configurations achieve sufficient decorrelation to warrant their consideration for use in a diversity system.

Acknowledgments

This work was completed at UCLA and supported by ARPA Contract DAAB07-93-C-C501. The contributions from M. A. Jensen and G. J. Pottie are gratefully acknowledged.

References

[1] M. A. Jensen and Y. Rahmat-Samii, IEEE Proc., Jan. 1995.

[2] J. S. Colburn, M. A. Jensen, G. J. Pottie and Y Rahmat-Samii, UCLA Technical Report ENG-95-133, 1995.

[3] D. Parsons, *The Mobile Radio Propagation Channel*, 1992.

[4] W. C. Lee, *Mobile Communications Engineering*, 1982.

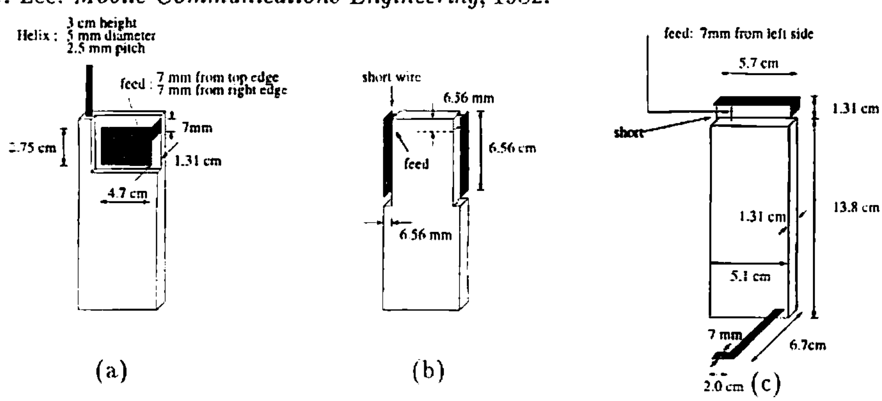

Figure 1: Handset antenna configurations considered: (a) top mounted helix and back mounted planar inverted F (PIFA); (b) side mounted PIFAs; (c) top mounted PIFA and "flip" monopole.

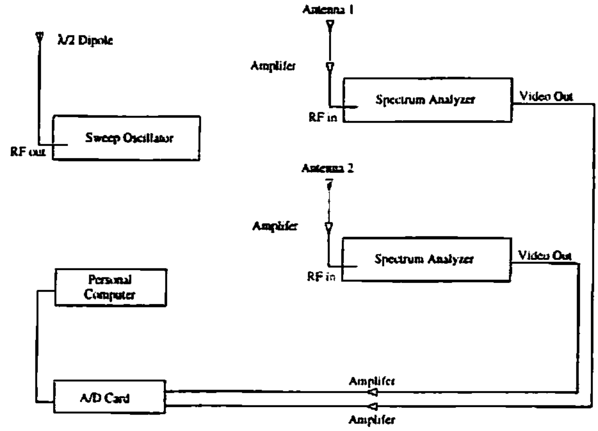

Figure 2: Equipment setup for antenna diversity measurements.

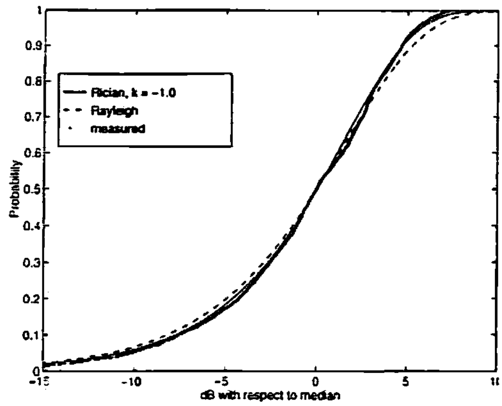

Figure 3: Measured, *best* fit Rician and Rayleigh comparison distribution for the "flip" monopole data set recorded on path 1.

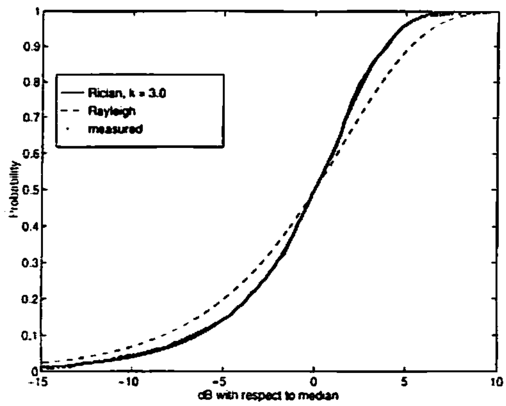

Figure 4: Measured, *best* fit Rician and Rayleigh comparison distribution for one of the 0.4 λ spaced dipole data sets recorded on path 2.

Table 1: Power correlation coefficients for the proposed antenna configurations. NA denotes data not available.

Antenna Configuration	Path 1	Path 4	Path 5	Path 6
0.06 λ separated dipole	0.8039	0.8089	0.7362	0.7521
0.4 λ separated dipole	0.6143	0.6281	0.5739	0.6226
side PIFAs	0.5100	0.5460	0.6053	0.5735
back PIFA/helix	0.6117	0.6182	0.5961	NA
top PIFA/flip monopole	0.5385	0.6586	0.6109	NA